



Published in final edited form as:

*Am J Sports Med.* 2019 July ; 47(8): 1844–1853. doi:10.1177/0363546519850165.

## Multiplanar Loading of the Knee and Its Influence on Anterior Cruciate Ligament and Medial Collateral Ligament Strain During Simulated Landings and Noncontact Tears

Nathaniel A. Bates, PhD<sup>\*,†,‡,§</sup>, Nathan D. Schilaty, DC, PhD<sup>†,‡,§</sup>, Christopher V. Nagelli, PhD<sup>‡</sup>, Aaron J. Krych, MD<sup>†,‡</sup>, Timothy E. Hewett, PhD<sup>†,‡,§,||</sup>

<sup>†</sup>Department of Orthopedic Surgery, Mayo Clinic, Rochester, Minnesota, USA.

<sup>‡</sup>Department of Biomedical Engineering and Physiology, Mayo Clinic, Rochester, Minnesota, USA.

<sup>§</sup>Sports Medicine Center, Mayo Clinic, Rochester, Minnesota, USA.

<sup>||</sup>Department of Physical Medicine and Rehabilitation, Mayo Clinic, Rochester, Minnesota, USA.

# These authors contributed equally to this work.

### Abstract

**Background:** Anterior cruciate ligament (ACL) tears and concomitant medial collateral ligament (MCL) injuries are known to occur during dynamic athletic tasks that place combinatorial frontal and transverse plane loads on the knee. A mechanical impact simulator that produces clinical presentation of ACL injury allows for the quantification of individual loading contributors leading to ACL failure.

**Purpose/Hypothesis:** The objective was to delineate the relationship between knee abduction moment, anterior tibial shear, and internal tibial rotation applied at the knee and ACL strain during physiologically defined simulations of impact at a knee flexion angle representative of initial contact landing from a jump. The hypothesis tested was that before ACL failure, abduction moment would induce greater change in ACL strain during landing than either anterior shear or internal rotation.

**Study Design:** Controlled laboratory study.

**Methods:** Nineteen cadaveric specimens were subjected to simulated landings in the mechanical impact simulator. During simulations, external knee abduction moment, internal tibial rotation moment, and anterior tibial shear loads were derived from a previously analyzed in vivo cohort and applied to the knee in varying magnitudes with respect to injury risk classification. Implanted strain gauges were used to track knee ligament displacement throughout simulation. Kruskal-Wallis tests were used to assess strain differences among loading factors, with Wilcoxon each pair post hoc tests used to assess differences of magnitude within each loading.

\*Address correspondence to Nathaniel A. Bates, Department of Orthopedic Surgery, Mayo Clinic, 200 First St SW, Rochester, MN 55902, USA (batesna@gmail.com).

Investigation performed at Mayo Clinic, Rochester, Minnesota, USA

For reprints and permission queries, please visit SAGE's Web site at <http://www.sagepub.com/journalsPermissions.nav>.

**Results:** Each loading factor significantly increased ACL strain ( $P < .005$ ). Within factors, the high-risk magnitude of each factor significantly increased ACL strain relative to the baseline condition ( $P = .002$ ). However, relative to knee abduction moment specifically, ACL strain increased with each increased risk magnitude ( $P = .015$ ).

**Conclusion:** Increased risk levels of each load factor contributed to increased levels of ACL strain during a simulated jump landing. The behavior of increased strain between levels of increased risk loading was most prevalent for changes in knee abduction moment. This behavior was observed in the ACL and MCL.

**Clinical Relevance:** Knee abduction moment may be the predominant precursor to ACL injury and concomitant MCL injury. As knee abduction occurs within the frontal plane, primary preventative focus should incorporate reduction of frontal plane knee loading in landing and cutting tasks, but secondary reduction of transverse plane loading could further increase intervention efficacy. Constraint of motion in these planes should restrict peak ACL strain magnitudes during athletic performance.

### Keywords

anterior cruciate ligament; landing; sports injury; knee; biomechanics; impact simulation

---

An estimated 250,000 anterior cruciate ligament (ACL) injuries occur annually in the United States,<sup>26</sup> with approximately 125,000 patients receiving ACL reconstruction,<sup>29</sup> for a net medical cost in excess of \$2 billion.<sup>5</sup> Despite the prevalence of ACL reconstruction treatment, only 55% to 88% of athletes <20 years of age return to sport after surgery, while only 53% of older patients subsequently return to sport.<sup>1,53,54</sup> Seven years after injury, only 36% still participated in their original sports.<sup>15</sup> One-quarter to one-third of those who do return are expected to incur a secondary ACL injury to the ipsilateral or contralateral limb.<sup>42,43,53,54</sup> This high second rupture rate may be attributable at least in part to alterations in knee response to combined internal tibial rotation (ITR) and knee abduction moments (KAMs) after ACL reconstruction, as anterior tibial translation is restored relative to the deficient state but overconstrained relative to the native knee, while peak transverse rotations are also underconstrained when the knee is near full extension.<sup>6</sup>

The ACL is known to provide 87% of the passive resistance to anterior translation in the knee,<sup>16,40</sup> as anterior tibial translation increases by a mean  $\pm$  SD  $18.2 \pm 4.4$  mm under 134 N of anterior tibial shear (ATS) in the ACL-deficient condition but only by  $4.2 \pm 1.6$  mm in an intact knee.<sup>6</sup> In addition, the ACL operates as a secondary restraint to ITR and KAM, as  $4^\circ$  of ITR added 0.5% strain and  $4^\circ$  of knee abduction rotation added 1.5% strain to the ligament.<sup>6-8,40</sup> Increased KAM during landing from a jump was specifically associated with an increased risk of ACL injury in an athletic population.<sup>25</sup> Also, as KAM is reduced through targeted neuromuscular interventions,<sup>20,22,55</sup> the risk of ACL injury across an athletic population was correspondingly found to decrease with these KAM-targeted interventions.<sup>21,24,52</sup> Specifically, KAM-targeted interventions have exhibited the greatest biomechanical changes and subsequent risk reduction on those athletes who exhibit the highest injury risk profiles, as determined by large KAM during landing.<sup>23</sup> Reduction of KAM was correlated with a 67% reduction in injury risk.<sup>24,52,55</sup> Despite these associations

between KAM and injury, the exact mechanism of ACL rupture remains controversial.<sup>44,48,49,56</sup>

In response to this controversy, a mechanical impact testing apparatus was developed to reliably elicit ACL ruptures on cadaveric specimens through the simulation of landing tasks over a physiologic time frame and thereby re-create the noncontact ACL injury mechanism in a controlled biomechanical laboratory environment.<sup>30</sup> This design was subsequently modified to enhance the physiologic accuracy of the simulation technique,<sup>10</sup> which resulted in a distribution of ACL injuries that was more accurately aligned to clinical presentation of the injury.<sup>11</sup> The mechanical impact simulator permits operators to control external loading parameters around the knee during landing, which consequently can be utilized to fill the gap in knowledge of which loads and combined loading mechanisms contribute greatest to ACL strain during simulated landings before ligament failure.

The objective of this investigation was to delineate the relationship between KAM, ATS, and ITR applied at the knee and ACL strain during physiologically defined simulations of landing tasks. The hypothesis tested was that before ACL failure, increased KAM would induce greater change in ACL strain during landing than either ATS or ITR.

## METHODS

This investigation was performed with the mechanical impact simulator, which has been detailed in the literature (Figure 1).<sup>9,10</sup> Briefly, 46 full lower extremity specimens obtained from an anatomic donations program (Anatomy Gifts Registry) were prepared and subjected to impact simulations. Specimens were resected of all skin and muscle tissue 3 cm proximal to the patella, with the quadriceps and hamstrings tendons intact. The femur was sectioned transversely 20 cm proximal to the patella. Each specimen was then inverted and potted into a custom fixture that was mounted on a 6-axis load cell (Omega 160 IP65/IP68; ATI Industrial Automation, Inc) such that the long axis of the femur was aligned with the vertical axis of the load cell. This load cell was oriented in 25° of flexion to represent the mean in vivo knee flexion angle at initial ground contact when athletes land from a 31-cm drop.<sup>3,10</sup> Pneumatic pistons (SMC Corporation) mounted to the load cell were then connected to the quadriceps and hamstrings tendons via cable clamps and carbon fiber rope ( $\text{Ø}^{7/64}$  in, Amsteel-Blue; Samson). A pulley system approximated the line of action of these carbon fiber ropes as close as possible to the orientation of the muscle bodies that correspond to each hamstrings and quadriceps tendon. Muscle forces were applied such that the overall quadriceps and hamstrings force were applied in an ideal 1:1 ratio with a magnitude of 450 N.<sup>33</sup> Muscle forces were constant throughout each simulation.

With the femur secured, the tibia was oriented vertically, and an 18.1-kg platform was rested on the sole of the foot. This platform represented the ground in our model and contained a uniaxial load cell (1720ACK-10kN; Interface, Inc) that was aligned with the heel of the foot through the long axis of the tibia. The uniaxial load cell represented the site of impulse delivery to the specimen and recorded the ground-reaction force generated for each impact. A compression clamp was secured to the shank of the specimen with a pair of carriage bolts that were drilled through the tibia. This custom clamp contained multiple attachment points

that were used to apply external loads to the knee joint. External loads included KAM, ATS, and ITR, each of which is known to contribute to ACL strain.<sup>8</sup> For the impactor model, these loads were applied via pneumatic pistons that attached to the tibial compression clamp with carbon fiber rope.

The magnitude of external KAM, ATS, and ITR was determined from previous in vivo kinetic analysis of 44 healthy athletes (mean  $\pm$  SD: age,  $23.3 \pm 4.1$  years; mass,  $72.6 \pm 13.9$  kg; height,  $172 \pm 10$  cm) who performed drop vertical jump tasks from a 31-cm box.<sup>10,11</sup> For each loading factor, the smallest peak magnitude generated by any athlete within the in vivo cohort was established as baseline risk. From there, the population was divided into groups based on population percentile for each loading factor. Loading percentiles were factor dependent and ranged from the 0th to 200th percentile of the observed population. Designations for these percentiles were baseline risk (<2nd percentile), low risk (~33rd percentile), moderate risk (~67th percentile), high risk (90th-100th percentile), and very high risk (200th percentile), as ACL injury risk classification is expected to divide an athletic population approximately into thirds.<sup>4,41</sup> The magnitude of loading that corresponds to each classification for each loading factor is displayed in Table 1, and all 26 potential loading combinations are displayed in Table 2. These kinetic loads were applied to the joint approximately 1 second before impulse delivery.

Impulse was delivered by a secondary 34.0-kg load sled that was suspended 31 cm above the ground platform with electromagnets. An electronic signal was used to cut power to the magnets and allow the sled to fall via gravity onto the ground platform. Slide rails were used to target the impulse delivery onto the uniaxial load cell within the ground platform.

Custom 3-mm microminiature differential variance resistance transducer (DVRT; LORD MicroStrain) strain gauges were implanted into the anteromedial bundle of the ACL and midsubstance of the medial collateral ligament (MCL) along the tibiofemoral joint line. DVRTs determined absolute ligament strain relative to the neutral position of the ligament, which was established following previously published methodologies.<sup>10,11,18,30,45</sup> Briefly, articulation of the tibia along a single line of action or about a single axis of rotation should allow an investigator to identify a voltage plateau where the DVRT becomes non-responsive. The inflection point that precedes this plateau should represent the neutral length of the ligament where the structure transitions from taut to lax. For the ACL, this inflection point determination was performed with an anterior/posterior drawer articulation of the tibia from its natural alignment at 25° of knee flexion.<sup>18</sup> For the MCL, this inflection point determination was performed with a pure abduction/adduction rotation articulation of the tibia from its natural alignment at 25° of knee flexion. Ligament strain can then be determined by  $(L_{DVRT}/L_N) \times 100 - 100$ , where  $L_{DVRT}$  is the instantaneous length of the DVRT and  $L_N$  is the length of the DVRT at the neutral position of the ligament. All data from the DVRTs, 6-axis load cell, and uniaxial load cell were collected with custom LabVIEW code (National Instruments Co) and sampled at 10,000 Hz. Data were then filtered through a low-pass, fourth-order Butterworth filter with a 12-Hz frequency. Custom MATLAB code (The MathWorks, Inc) was then used to identify the instant of impulse delivery for each impact and interpolate data from this point of initial contact for a 1-second duration into 301 points for statistical analysis.

Once specimens were secured within the mechanical impact simulator, they were subjected to a series of up to 26 impact simulations where the combinatorial magnitudes of KAM, ATS, and ITR specified in Table 2 were applied to the joint in a randomized order. Previous literature on the mechanical impact simulator has indicated that the externally applied KAM, ATS, and ITR loads were separated into tertiles based on joint load estimates calculated from the aforementioned *in vivo* cohort.<sup>10,11,32,48,49</sup> However, data from uniaxial load cells (MLP-300, MLP-1K, and SWO-2K; Transducer Techniques) mounted on each pneumatic piston revealed that these estimated inputs were realized in the magnitudes indicated in Table 1. Both the anticipated- and realized-loading stratifications represent a diversity of low, moderate, and high-risk landing simulations enacted on the cadaveric specimens.<sup>34</sup> Testing was terminated once the specimen suffered a hard tissue disruption (tibial or femoral fracture) or soft tissue disruption (nonelastic ligamentous response from the ACL) on the macroscopic level.<sup>10</sup> Of the 46 specimens tested, 19 specimens (age,  $39.1 \pm 8.9$  years; mass,  $93.6 \pm 22.5$  kg; height,  $175.9 \pm 8.6$  cm; 15 males, 4 females) completed the full impact protocol before sustaining a hard or soft tissue injury. As DVRT-measured interspecimen variability for ligament strain is known to be high,<sup>7,11,14</sup> only these specimens that completed the testing protocol without sustaining prior injury were included in the statistical analysis to avoid confounding effects.

Statistical analysis was performed with a Kruskal-Wallis test where KAM, ATS, and ITR were the 3 factors. Within each factor, there were either 2 or 4 magnitudes of loading, which were determined by the level of injury risk (baseline, low, moderate, high, or very high risk). Risk levels were assessed within each load factor independent of the combined loading that was simultaneous applied from the remaining 2 load factors. These within-factor differences were determined by Wilcoxon each pair post hoc analysis. For all statistical analysis, significance was set at  $\alpha < .05$ .

## RESULTS

### ACL Strain

Relative to absolute ACL strain in the Kruskal-Wallis model, KAM, ATS, and ITR were all significant factors ( $P < .005$ ). Post hoc analysis between risk levels within each loading factor revealed significant differences for each KAM, ATS, and ITR. Within KAM, very-high-risk magnitudes produced greater peak ACL strain than all other conditions ( $P < .001$ ). Also, high-risk KAM produced greater ACL strain than baseline-risk KAM ( $P = .009$ ) (Figures 2 and 3). High-risk ATS simulations produced greater ACL strain than baseline-risk ATS ( $P = .002$ ). Baseline-risk ITR simulations produced lower ACL strain than all other magnitudes of ITR ( $P = .037$ ). High-risk ITR simulations approached significance relative to low- and moderate-risk ITR ( $P = .058$  and  $.062$ ).

Relative to  $\Delta$ ACL strain from baseline in the Kruskal-Wallis model, KAM, ATS, and ITR were all significant factors ( $P < .001$ ). Post hoc analysis between risk levels within each loading factor revealed significant differences for each KAM, ATS, and ITR. All simulated risk levels of KAM produced significantly different  $\Delta$ ACL strain, and  $\Delta$ ACL strain increased as risk level increased ( $P = .044$ ) (Figures 2 and 3). High-risk ATS simulations

produced greater  $\Delta$ ACL strain than baseline-risk ATS ( $P < .002$ ). High-risk ITR simulations produced greater  $\Delta$ ACL strain than all other magnitudes of ITR ( $P < .045$ ).

### MCL Strain

Across all trials, peak MCL strain was not significantly correlated with peak ACL strain ( $P = .103$ ;  $r^2 = 0.01$ ). Relative to absolute MCL strain in the Kruskal-Wallis model, KAM, ATS, and ITR were all significant ( $P = .006$ ). With the exception of moderate risk relative to baseline risk ( $P = .149$ ), all simulated risk levels of KAM produced significantly different peak MCL strains, as strain increased with increased risk levels ( $P = .001$ ) (Figures 4 and 5). High-risk ATS simulations produced significantly greater peak MCL strain than baseline-risk ATS simulations ( $P = .022$ ). High-risk ITR simulations exhibited greater peak MCL strain than baseline-risk ITR simulations ( $P = .018$ ).

Across all trials, DMCL strain was significantly correlated with  $\Delta$ ACL strain but accounted for only 4% of the variance in the linear model ( $P < .001$ ;  $r^2 = 0.04$ ). Relative to DMCL strain from baseline in the Kruskal-Wallis model, KAM was again significant ( $P < .001$ ), while ATS and ITR were not ( $P = .186$  and  $.329$ , respectively). Within factors, DMCL strain increased with each risk level of KAM ( $P < .001$ ) (Figures 4 and 5), with the exception of baseline- to moderate-risk KAM ( $P = .375$ ). There was no differences in  $\Delta$ MCL strain between risk levels of ATS and ITR ( $P = .083$ ).

## DISCUSSION

The current findings support the stated hypothesis that KAM would induce greater change in ACL strain during landing with the knee at  $25^\circ$  of flexion than either ATS or ITR in the cadaveric model. Compared with ITR—with which only the baseline- and high-risk level of magnitude expressed significant changes in ACL strain—KAM exhibited significant differences in ACL strain at each risk level examined. KAM was especially influential in simulations with very-high-risk loading, where the mean peak ACL strain was 1.5 times greater than in baseline-risk simulations and the mean  $\Delta$ ACL strain was nearly double that of baseline-risk trials. Furthermore, as demonstrated in Figure 4, KAM was the only external loading factor to exhibit a distinctly positive slope correlated with increased load magnitude along the single-factor axis. This indicates that KAM is the main influence of the strain increase observed in the ACL in this model. For ATS and ITR, the slope increase primarily appeared on the combinatorial axis as external load intensity increased. This behavior indicates that the combinatorial loads had a greater effect on the ACL than did ATS or ITR in the cadaveric model, and it supports the assessment that KAM was the primary driving factor behind increasing ACL strains in this investigation.

KAM was previously associated with ACL loading in vitro and with predisposition for ACL injury in vivo.<sup>8,9,25,28</sup> Within an adolescent athletic population, 25.25 Nm of frontal plane torque at the knee when landing from a 31-cm drop was determined as the threshold for high-injury risk.<sup>35</sup> Subsequently, a series of measures and evaluations were designed to rapidly parse out the presence of this threshold in a clinical setting without the use of arduous and expensive 3-dimensional motion analysis laboratory measures.<sup>36–39</sup> While predictive of potential injury risk, this KAM threshold was established among healthy



athletes during a controlled landing task where no injuries occurred and risk for injury in an athletic population was near zero.<sup>25</sup> As such, it was expected that external KAM loads in the current experiment would need to exceed this threshold, potentially significantly, to induce ACL injury in the cadaveric specimens. Within the examined in vivo population, the final tertile exceeded the established threshold and adhered to the rule of thirds.<sup>4,41</sup> For this experiment, a very high loading classification was created, at double the maximum KAM load observed in vivo, since the in vivo loads induced no in vivo injuries.

While some of the literature corroborates KAM as a loading and injury risk mechanism for the ACL, contradictory data exist. DVRTs implanted into live-participant ACLs exhibited minimal changes in ACL strain during weight-bearing and nonweightbearing trials where knees were passively articulated  $\pm 15$  N m of varus-valgus torque while maintaining 20° of knee flexion.<sup>19</sup> However, it is important to consider the parameters of this prior in vivo work within the context of the present study. A 15-N m frontal plane torque is inferior to both the high-risk in vivo ACL injury risk threshold<sup>25</sup> and the moderate-risk KAM applied by the mechanical impact simulator. As documented in the results, differences between the baseline- and moderate-risk KAM simulations lacked significance; therefore, it is unsurprising that 15-N m torques lacked significance in vivo. In addition, the in vivo weight-bearing reported in the literature was 40% bodyweight,<sup>19</sup> whereas the mechanical impact simulator mimics landing from a jump, which applies approximately 225% bodyweight per limb.<sup>2,10</sup> Accordingly, the application of increased magnitudes during the in vivo study may have also established significance, but limitations presented by the need to protect live participants from injury are understood.

Maximal load and strain on the ACL during simulated testing occurred when combined rotational forces were applied to the knee joint.<sup>8,51</sup> This has empirically been appreciated by clinicians, as the pivot-shift test to evaluate ACL integrity was established per the principle of coupling ITR with KAM to diagnose ACL insufficiency and is the clinical test that exhibits the greatest specificity.<sup>13</sup> Quantifiably, the mechanical application of 5-N m ITR with 10-N m KAM to a cadaveric knee introduced significantly greater subluxation in the same specimen between 0° and 60° of flexion in an ACL-deficient state than in an ACL-intact state.<sup>17</sup> Furthermore, a multitude of robotics simulations have examined kinematic and kinetic response to the application of 5 N m of ITR combined with 7 to 10 N m of KAM.<sup>6</sup> In these studies, the application of 10-N m KAM as opposed to 7-N m KAM elicited significantly greater anterior tibial translation between 15° and 45° of knee flexion and greater ligament force between 0° and 45° of knee flexion. During computerized simulation, combined KAM and ITR produced a peak strain of ~11.5% on the ACL, whereas isolated KAM induced a peak strain of ~7.75% and isolated ITR, ~7.0%.<sup>51</sup> Like-wise, applications of KAM and ITR constrained to 4° of kinematic rotation on intact cadaveric knees found that isolated ITR induced a 0.5% increase in ACL strain, isolated KAM induced a 1.5% increase, and combined rotations induced a 1.9% increase relative to the starting position ACL strain.<sup>8</sup> These prior investigations each corroborate the findings of the current study that KAM and ITR exhibit an additive effect of influence on ACL strain but KAM individually drives a larger portion of this additive effect.

A prior impact-driven simulator was also able to render ACL injuries on 88% of cadaveric specimens tested; however, two-thirds of these injuries presented at the tibial plateau.<sup>28,30,45</sup> Tibial plateau ruptures are the least common clinical presentation of ACL injuries among postpubertal patients.<sup>11</sup> As with the present mechanical impact simulator, this prior device applied KAM, ATS, and ITR to each specimen before an impulse load was delivered. The magnitude of these external loads was based on in silico simulation models of ACL failure and ranged from 0 to 150 N m of KAM, 0 to 268 N of ATS, and 0 to 80 N m of ITR.<sup>28,50</sup> This prior model showed that within each external load variable, the highest applied magnitude increased ACL strain during impact relative to baseline.<sup>28</sup> In the present mechanical impact simulator, external loads were established relative to healthy landings kinetics from an in vivo cohort, and subsequently, the peak magnitudes applied for each factor were lower than those from the prior device. Despite this, ACL strain for the high- and very-high-risk load applications was significant relative to the baseline simulations. Unlike the prior device, KAM exhibited significant increases in ACL strain at every interval in the investigation, as opposed to just between the baseline and maximal magnitudes. Part of this difference may be attributed to the more instantaneous delivery of external loads in the mechanical impact simulator with the use of pneumatic pistons.<sup>10</sup> The adaptation of pneumatics presented a more physiologically representative load delivery to the specimen than the hanging weight that was used in the prior simulator. Despite differences in load applications, both simulators demonstrated that the greatest ACL strain was attained under multiple applied external loads, which indicates that KAM, ATS, and ITR have a combinatorial effect on ACL load and injury risk. This concept is corroborated by prior in silico and in vitro robotics modeling.<sup>6,8,27,50,51</sup>

Within the mechanical impact simulator, it was documented that the peak ACL strain ( $15.3\% \pm 8.7\%$ ) before an ACL failure event was approximately 3 times that of the peak MCL strain ( $5.1\% \pm 5.6\%$ ).<sup>11</sup> This finding corroborates previous impact- and robotically driven simulations of landing tasks, where the MCL bore significantly less load than the ACL and subsequently played a relatively diminished role in joint constraint during this standard athletic task.<sup>9,45</sup> Despite the lower strain exhibited in the MCL than the ACL in the present study, the clinical ratio of concomitant MCL injuries that occurred in approximately a third of ACL injuries was maintained in the mechanical impact simulator.<sup>11</sup> Further investigation is necessary to determine whether the concomitant MCL injuries result from an instantaneous redistribution of load into the MCL immediately after ACL rupture or simply a heightened normative load acceptance of the MCL in the concomitantly injured specimens.<sup>47</sup> In addition, if the MCL exhibits any laxity within the knee, the ACL will see greater loads,<sup>12</sup> which clinically supports the potential of an ACL rupture without concomitant MCL failure.

One limitation of the current investigation is that quadriceps and hamstrings muscle contractions were constant throughout the simulation. In vivo, these muscle contractions vary throughout the performance of a motion task.<sup>31,46</sup> Assessment of specific muscular contributions to joint restraint was outside the scope of the current project, and the muscle contractions applied were primarily to stabilize the joint during landing. For this reason, the quadriceps and hamstrings forces were applied in a 1:1 ratio, which is ideal for protection of the ACL.<sup>33</sup> Further study is warranted to understand how higher-risk muscular ratios and



matched physiologic contraction timing influence the intra-articular mechanical response. Because of methodological complications with the pneumatic pistons, only 2 levels of ATS loading were successfully simulated from the in vivo cohort. However, the levels represented were the baseline- and high-risk classifications, which still depicted the high and low ends of the population spectrum but did not divide the population into tertiles as originally intended. As cited in the previously published methodology literature, preconditioning impacts were run before testing to minimize viscoelastic effects.<sup>10</sup> However, it remains possible that the ACL and MCL fibers experienced nonelastic stretching during testing before documented failure. Given the nature of the experiments performed, evaluation of isolated ligament mechanics pre- and posttesting was not possible; therefore, potential ligament stretch was not presently evaluated. If such behavior occurred, it would potentially alter the point at which a ligament engaged its taut length at lower strains, but it should not obscure the peak strain attained in a trial, as the DVRT remained implanted and would continue to reference the initial zero strain length. Finally, knee flexion angle in the present simulation is restrained at 25° of flexion.<sup>10</sup> This orientation agrees with the average flexion at initial contact during landing,<sup>3</sup> aligns with estimates of ACL injury occurring within 50 milliseconds of contact that would permit only limited knee flexion,<sup>31</sup> and supports the postulate that flat-footed landings with an extended knee are a precursor to ACL rupture.<sup>24–26</sup> However, live athletes would have the potential ability to further flex their knees upon landing, which was precluded from the current specimens.

## CONCLUSION

Increased risk levels of KAM, ATS, and ITR each contributed to increased levels of ACL strain during a simulated jump landing where impulse is induced at 25° of knee flexion in a cadaveric model. However, KAM exhibited the most significant behavior of increased strain between levels of increased risk loading applied to the specimens. This responsive behavior was observed in both the ACL and the MCL. Subsequently, KAM is likely the predominant precursor to ACL injury and concomitant MCL injury. Therefore, preventative programs should continue to focus on the reduction of frontal plane knee motion and loads in unanticipated landing and cutting tasks. However, a multiplanar approach that restricts loading within the frontal plane and secondarily restricts loading within the transverse plane is likely to influence the most efficacious reduction in ACL injury incidence.

## Acknowledgments

One or more of the authors has declared the following potential conflict of interest or source of funding: Funding was provided by National Institutes of Health grants from the National Institute of Arthritis and Musculoskeletal and Skin Diseases (R01-AR056259, R01-AR055563 K12-HD065987, T32-AR56950, and L30-AR070273). A.J.K. is a paid consultant for Arthrex Inc and DePuy Orthopedics Inc, receives royalties for meniscus repair from Arthrex Inc, and has received honoraria from Vericel Corp and MTF. AOSSM checks author disclosures against the Open Payments Database (OPD). AOSSM has not conducted an independent investigation on the OPD and disclaims any liability or responsibility relating thereto.

## REFERENCES

1. Ardern CL, Taylor NF, Feller JA, Webster KE. Fifty-five per cent return to competitive sport following anterior cruciate ligament reconstruction surgery: an updated systematic review and meta-

- analysis including aspects of physical functioning and contextual factors. *Br J Sports Med.* 2014;48(21):1543–1552. [PubMed: 25157180]
2. Bates NA, Ford KR, Myer GD, Hewett TE. Impact differences in ground reaction force and center of mass between the first and second landing phases of a drop vertical jump and their implications for injury risk assessment. *J Biomech.* 2013;46(7):1237–1241. [PubMed: 23538000]
  3. Bates NA, Ford KR, Myer GD, Hewett TE. Kinetic and kinematic differences between first and second landings of a drop vertical jump task: implications for injury risk assessments. *Clin Biomech (Bristol, Avon).* 2013;28(4):459–466.
  4. Bates NA, Hewett TE. Motion analysis and the anterior cruciate ligament: classification of injury risk. *J Knee Surg.* 2016;29(2):117–125. [PubMed: 26383143]
  5. Bates NA, McPherson AL, Rao MB, Myer GD, Hewett TE. Characteristics of inpatient anterior cruciate ligament reconstructions and concomitant injuries. *Knee Surg Sports Traumatol Arthrosc.* 2016;24(9):2778–2786. [PubMed: 25510363]
  6. Bates NA, Myer GD, Shearn JT, Hewett TE. Anterior cruciate ligament biomechanics during robotic and mechanical simulations of physiologic and clinical motion tasks: a systematic review and meta-analysis. *Clin Biomech (Bristol, Avon).* 2015;30(1):1–13.
  7. Bates NA, Nesbitt RJ, Shearn JT, Myer GD, Hewett TE. The influence of internal and external tibial rotation offsets on knee joint and ligament biomechanics during simulated athletic tasks. *Clin Biomech (Bristol, Avon).* 2018;52:109–116.
  8. Bates NA, Nesbitt RJ, Shearn JT, Myer GD, Hewett TE. Knee abduction affects greater magnitude of change in ACL and MCL strains than matched internal tibial rotation in vitro. *Clin Orthop Relat Res.* 2017;475:2385–2396. [PubMed: 28455730]
  9. Bates NA, Nesbitt RJ, Shearn JT, Myer GD, Hewett TE. Relative strain in the anterior cruciate ligament and medial collateral ligament during simulated jump landing and sidestep cutting tasks: implications for injury risk. *Am J Sports Med.* 2015;43(9):2259–2269. [PubMed: 26150588]
  10. Bates NA, Schilaty ND, Nagelli CV, Krych AJ, Hewett TE. Novel mechanical impact simulator designed to generate clinically relevant anterior cruciate ligament ruptures. *Clin Biomech (Bristol, Avon).* 2017;44:36–44.
  11. Bates NA, Schilaty ND, Nagelli CV, Krych AJ, Hewett TE. Validation of non-contact anterior cruciate ligament tears produced by a mechanical impact simulator against the clinical presentation of injury. *Am J Sports Med.* 2018;46(9):2113–2121. [PubMed: 29864374]
  12. Battaglia MJ 2nd, Lenhoff MW, Ehteshami JR, et al. Medial collateral ligament injuries and subsequent load on the anterior cruciate ligament: a biomechanical evaluation in a cadaveric model. *Am J Sports Med.* 2009;37(2):305–311. [PubMed: 19098154]
  13. Benjaminse A, Gokeler A, van der Schans CP. Clinical diagnosis of an anterior cruciate ligament rupture: a meta-analysis. *J Orthop Sports Phys Ther.* 2006;36(5):267–288. [PubMed: 16715828]
  14. Beynnon B, Howe JG, Pope MH, Johnson RJ, Fleming BC. The measurement of anterior cruciate ligament strain in vivo. *Int Orthop.* 1992;16(1):1–12. [PubMed: 1572761]
  15. Brophy RH, Schmitz L, Wright RW, et al. Return to play and future ACL injury risk after ACL reconstruction in soccer athletes from the Multicenter Orthopaedic Outcomes Network (MOON) group. *Am J Sports Med.* 2012;40(11):2517–2522. [PubMed: 23002201]
  16. Butler DL, Noyes FR, Grood ES. Ligamentous restraints to anteriorposterior drawer in the human knee: a biomechanical study. *J Bone Joint Surg Am.* 1980;62(2):259–270. [PubMed: 7358757]
  17. Engebretsen L, Wijdicks CA, Anderson CJ, Westerhaus B, LaPrade RF. Evaluation of a simulated pivot shift test: a biomechanical study. *Knee Surg Sports Traumatol Arthrosc.* 2012;20(4):698–702. [PubMed: 22057355]
  18. Fleming BC, Beynnon BD, Tohyama H, et al. Determination of a zero strain reference for the anteromedial band of the anterior cruciate ligament. *J Orthop Res.* 1994;12:789–795. [PubMed: 7983554]
  19. Fleming BC, Renstrom PA, Beynnon BD, et al. The effect of weight bearing and external loading on anterior cruciate ligament strain. *J Biomech.* 2001;34:163–170. [PubMed: 11165279]
  20. Ford KR, Nguyen AD, Dischiavi SL, Hegedus EJ, Zuk EF, Taylor JB. An evidence-based review of hip-focused neuromuscular exercise interventions to address dynamic lower extremity valgus. *Open Access J Sports Med.* 2015;6:291–303. [PubMed: 26346471]

21. Hewett TE, Ford KR, Myer GD. Anterior cruciate ligament injuries in female athletes: part 2. A meta-analysis of neuromuscular interventions aimed at injury prevention. *Am J Sports Med.* 2006;34(3):490–498. [PubMed: 16382007]
22. Hewett TE, Ford KR, Xu YY, Khoury J, Myer GD. Effectiveness of neuromuscular training based on the neuromuscular risk profile. *Am J Sports Med.* 2017;45(9):2142–2147. [PubMed: 28441059]
23. Hewett TE, Ford KR, Xu YY, Khoury J, Myer GD. Utilization of ACL injury biomechanical and neuromuscular risk profile analysis to determine the effectiveness of neuromuscular training. *Am J Sports Med.* 2016;44(12):3146–3151. [PubMed: 27474385]
24. Hewett TE, Lindenfeld TN, Riccobene JV, Noyes FR. The effect of neuromuscular training on the incidence of knee injury in female athletes: a prospective study. *Am J Sports Med.* 1999;27(6): 699–706. [PubMed: 10569353]
25. Hewett TE, Myer GD, Ford KR, et al. Biomechanical measures of neuromuscular control and valgus loading of the knee predict anterior cruciate ligament injury risk in female athletes: a prospective study. *Am J Sports Med.* 2005;33(4):492–501. [PubMed: 15722287]
26. Johnson DL, Warner JJP. Diagnosis for anterior cruciate ligament surgery. *Clin Sports Med.* 1993;12(4):671–684. [PubMed: 8261519]
27. Kiapour A, Kiapour AM, Kaul V, et al. Finite element model of the knee for investigation of injury mechanisms: development and validation. *J Biomech Eng.* 2014;136(1):011002.
28. Kiapour AM, Demetropoulos CK, Kiapour A, et al. Strain response of the anterior cruciate ligament to uniplanar and multiplanar loads during simulated landings: implications for injury mechanism. *Am J Sports Med.* 2016;44(8):2087–2096. [PubMed: 27159285]
29. Kim SJ, Choi DH, Mei Y, Hwang BY. Does physiologic posterolateral laxity influence clinical outcomes of anterior cruciate ligament reconstruction? *J Bone Joint Surg Am.* 2011;93(21):2010–2014. [PubMed: 22048096]
30. Levine JW, Kiapour AM, Quatman CE, et al. Clinically relevant injury patterns after an anterior cruciate ligament injury provide insight into injury mechanisms. *Am J Sports Med.* 2013;41(2): 385–395. [PubMed: 23144366]
31. McNitt-Gray JL, Hester DME, Mathiyakom W, Munkasy BA. Mechanical demand on multijoint control during landing depend on orientation of the body segments relative to the reaction force. *J Biomech.* 2001;34:1471–1482. [PubMed: 11672722]
32. McPherson AL, Bates NA, Schilaty ND, Nagelli CV, Krych AJ, Hewett TE. Ligament strain response between lower extremity contralateral pairs during in vitro landing simulation. *Orthop J Sports Med.* 2018;6(4):2325967118765978.
33. Myer GD, Ford KR, Barber Foss KD, Liu C, Nick TG, Hewett TE. The relationship of hamstrings and quadriceps strength to anterior cruciate ligament injury in female athletes. *Clin J Sport Med.* 2009;19(1):3–8. [PubMed: 19124976]
34. Myer GD, Ford KR, Di Stasi SL, Foss KD, Micheli LJ, Hewett TE. High knee abduction moments are common risk factors for patellofemoral pain (PFP) and anterior cruciate ligament (ACL) injury in girls: is PFP itself a predictor for subsequent ACL injury? *Br J Sports Med.* 2015;49(2):118–122. [PubMed: 24687011]
35. Myer GD, Ford KR, Foss KD, Rauh MJ, Paterno MV, Hewett TE. A predictive model to estimate knee-abduction moment: implications for development of a clinically applicable patellofemoral pain screening tool in female athletes. *J Athl Train.* 2014;49(3):389–398. [PubMed: 24762234]
36. Myer GD, Ford KR, Hewett TE. New method to identify athletes at high risk of ACL injury using clinic-based measurements and free-ware computer analysis. *Br J Sports Med.* 2011;45(4):238–244. [PubMed: 21081640]
37. Myer GD, Ford KR, Khoury J, Hewett TE. Three-dimensional motion analysis validation of a clinic-based nomogram designed to identify high ACL injury risk in female athletes. *Phys Sports med.* 2011;39(1): 19–28.
38. Myer GD, Ford KR, Khoury J, Succop P, Hewett TE. Clinical correlates to laboratory measures for use in non-contact anterior cruciate ligament injury risk prediction algorithm. *Clin Biomech (Bristol, Avon).* 2010;25(7):693–699.

39. Myer GD, Ford KR, Khoury J, Succop P, Hewett TE. Development and validation of a clinic-based prediction tool to identify female athletes at high risk for anterior cruciate ligament injury. *Am J Sports Med.* 2010;38(10):2025–2033. [PubMed: 20595554]
40. Nesbitt RJ, Herfat ST, Boguszewski DV, Engel AJ, Galloway MT, Shearn JT. Primary and secondary restraints of human and ovine knees for simulated in vivo gait kinematics. *J Biomech.* 2014; 47(9):2022–2027. [PubMed: 24326097]
41. Noyes FR, McGinniss GH, Mooar LA. Functional disability in the anterior cruciate insufficient knee syndrome: review of knee rating systems and projected risk factors in determining treatment. *Sports Med.* 1984;1:278–302. [PubMed: 6390605]
42. Paterno MV, Rauh MJ, Schmitt LC, Ford KR, Hewett TE. Incidence of contralateral and ipsilateral anterior cruciate ligament (ACL) injury after primary ACL reconstruction and return to sport. *Clin J Sport Med.* 2012;22(2):116–121. [PubMed: 22343967]
43. Paterno MV, Schmitt LC, Ford KR, et al. Biomechanical measures during landing and postural stability predict second anterior cruciate ligament injury after anterior cruciate ligament reconstruction and return to sport. *Am J Sports Med.* 2010;38(10):1968–1978. [PubMed: 20702858]
44. Quatman CE, Hewett TE. The anterior cruciate ligament injury controversy: is “valgus collapse” a sex-specific mechanism? *Br J Sports Med.* 2009;43(5):328–335. [PubMed: 19372087]
45. Quatman CE, Kiapour AM, Demetropoulos CK, et al. Preferential loading of the ACL compared with the MCL during landing: a novel in sim approach yields the multiplanar mechanism of dynamic valgus during ACL injuries. *Am J Sports Med.* 2014;42(1):177–186. [PubMed: 24124198]
46. Russell PJ, Croce RV, Swartz EE, Decoster LC. Knee-muscle activation during landings: developmental and gender comparisons. *Med Sci Sports Exerc.* 2007;39(1):159–170. [PubMed: 17218898]
47. Schilaty ND, Bates NA, Krych AJ, Hewett TE. Frontal plane medial collateral ligament strain characteristics concurrent to anterior cruciate ligament failure. *Am J Sports Med.* In press. doi: 10.1177/0363546519854286
48. Schilaty ND, Bates NA, Nagelli C, Krych AJ, Hewett TE. Sex differences of medial collateral and anterior cruciate ligament strains with cadaveric impact simulations. *Orthop J Sports Med.* 2018; 6(4):2325967118765215.
49. Schilaty ND, Bates NA, Nagelli CV, Krych AJ, Hewett TE. Sex differences of knee kinetics that occur with anterior cruciate ligament strain on cadaveric impact simulations. *Orthop J Sports Med.* 2018;6(3):2325967118761037.
50. Shin CS, Chaudhari AM, Andriacchi TP. The influence of deceleration forces on ACL strain during single-leg landing: a simulation study. *J Biomech.* 2007;40(5):1145–1152. [PubMed: 16797556]
51. Shin CS, Chaudhari AM, Andriacchi TP. Valgus plus internal rotation moments increase anterior cruciate ligament strain more than either alone. *Med Sci Sports Exerc.* 2011;43(8):1484–1491. [PubMed: 21266934]
52. Sugimoto D, Myer GD, McKeon JM, Hewett TE. Evaluation of the effectiveness of neuromuscular training to reduce anterior cruciate ligament injury in female athletes: a critical review of relative risk reduction and numbers-needed-to-treat analyses. *Br J Sports Med.* 2012;46(14):979–988. [PubMed: 22745221]
53. Webster KE, Feller JA. Exploring the high reinjury rate in younger patients undergoing anterior cruciate ligament reconstruction. *Am J Sports Med.* 2016;44(11):2827–2832. [PubMed: 27390346]
54. Webster KE, Feller JA, Leigh WB, Richmond AK. Younger patients are at increased risk for graft rupture and contralateral injury after anterior cruciate ligament reconstruction. *Am J Sports Med.* 2014;42(3):641–647. [PubMed: 24451111]
55. Webster KE, Hewett TE. A meta-analysis of meta-analyses of anterior cruciate ligament injury reduction training programs. *J Orthop Res.* 2018;36(10):2696–2708. [PubMed: 29737024]
56. Yu B, Garrett WE. Mechanisms of non-contact ACL injuries. *Br J Sports Med.* 2007;41(suppl 1):i47–i51. [PubMed: 17646249]

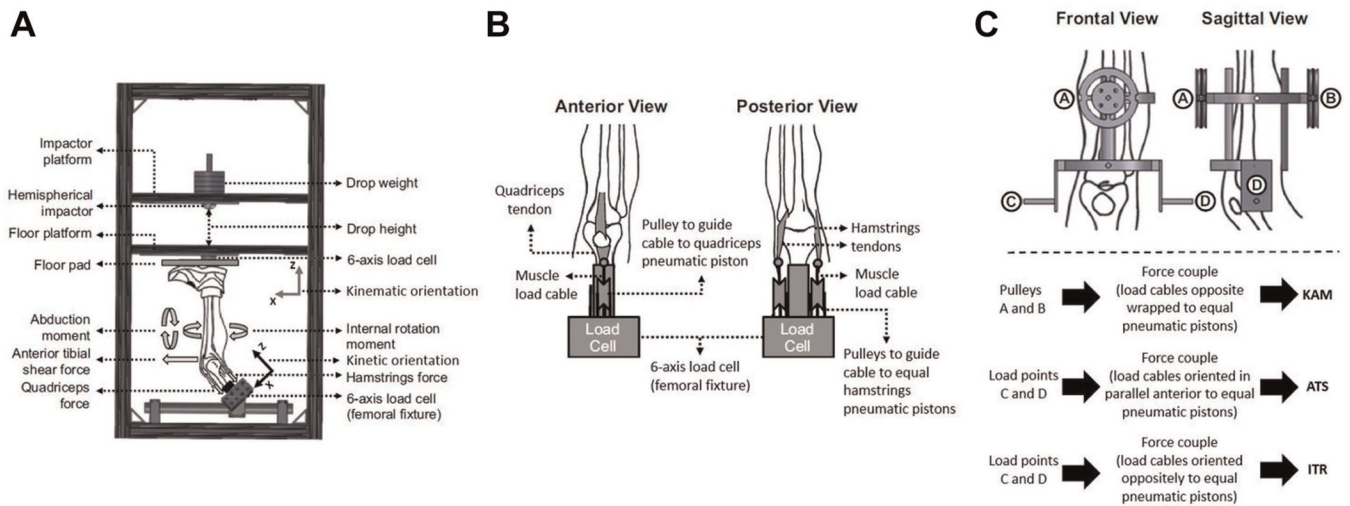


**Figure 1.** (A) Metaview of custom designed mechanical impact simulator for creation of ACL ruptures.<sup>10</sup> (B) Cable pulley system used to deliver pneumatically actuated loads to the quadriceps and hamstrings tendons. (C) External fixation frame attached to the tibia and used to deliver pneumatically actuated KAM, ATS, and ITR loads to each specimen. ACL, anterior cruciate ligament; ATS, anterior tibial shear; ITR, internal tibial rotation; KAM, knee abduction moment. This figure has been reproduced from Bates et al (2018, *Am J Sports Med*).<sup>11,28</sup>

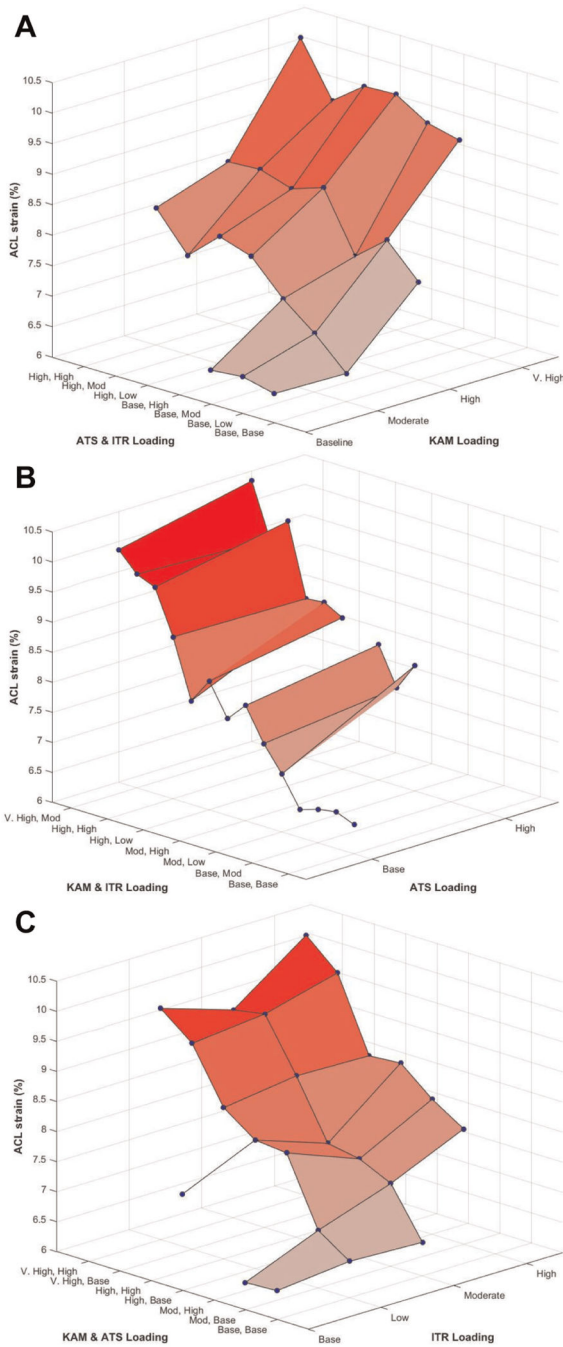


**Figure 2.** Heat maps that depict how (A) KAM, (B) ATS, and (C) ITR individually influence absolute ACL strain relative to each combination of the other 2 loading conditions. The highest strain is observed when all 3 conditions are combined in their highest-risk states. Note that for each plot, the effect of the isolated loading factor is observed along the tertiary ( $y$ ) axis, while the remaining combinatorial loading is depicted along the primary ( $x$ ) axis. Moving from left to right along the tertiary axis on each plot, KAM affects a steeper increase in



strain than ATS or ITR. ACL, anterior cruciate ligament; ATS, anterior tibial shear; ITR, internal tibial rotation; KAM, knee abduction moment.

Author Manuscript

Author Manuscript

Author Manuscript

Author Manuscript

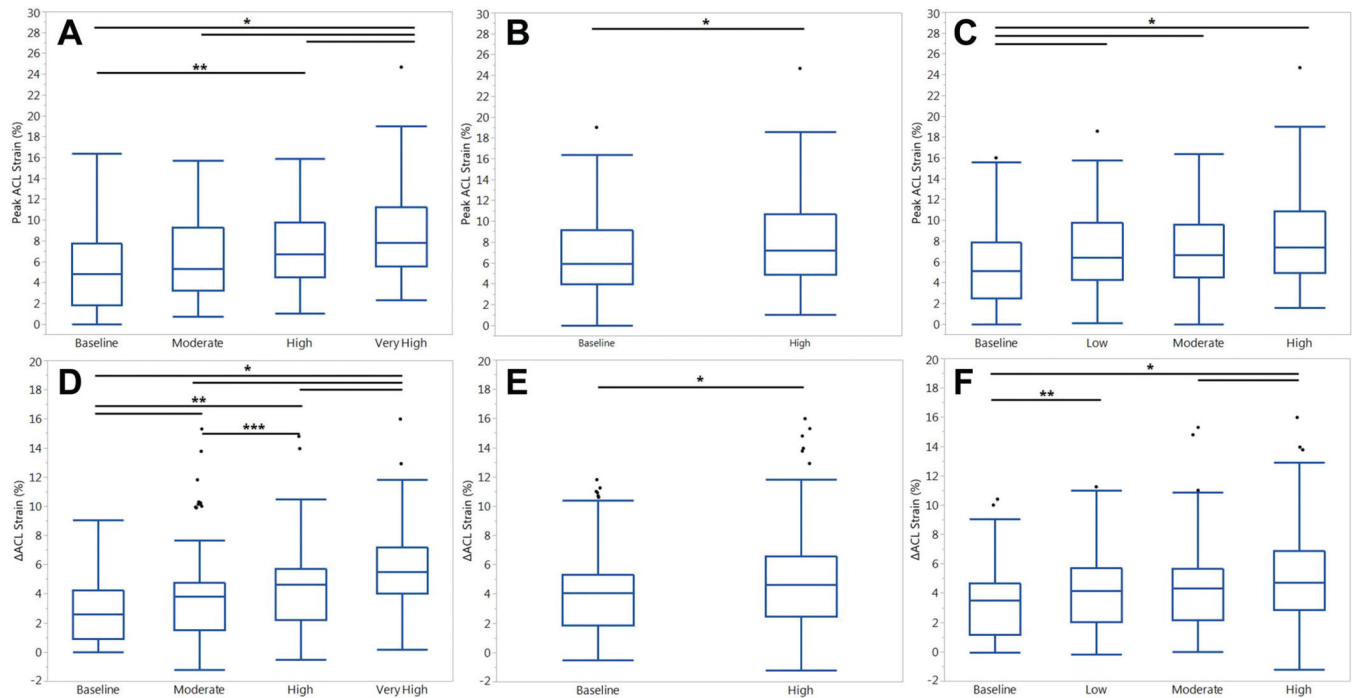


**Figure 3.**

Box plots with medians and interquartile ranges for peak ACL strain from all trials, separated by risk level for each loading factor: (A) KAM, (B) ATS, and (C) ITR. Means and SDs for  $\Delta$ ACL strain from all trials, separated by risk level for each loading factor: (D) KAM, (E) ATS, and (F) ITR. Horizontal bars at the superior aspect of the graph indicate significant difference ( $P < .05$ ) between the 2 indicated risk levels. Error bars indicate 95% CI, and circles indicate outliers. \* $P < .05$ . \*\* $P < .01$ . \*\*\* $P < .001$ . ACL, anterior cruciate ligament; ATS, anterior tibial shear; ITR, internal tibial rotation; KAM, knee abduction moment.

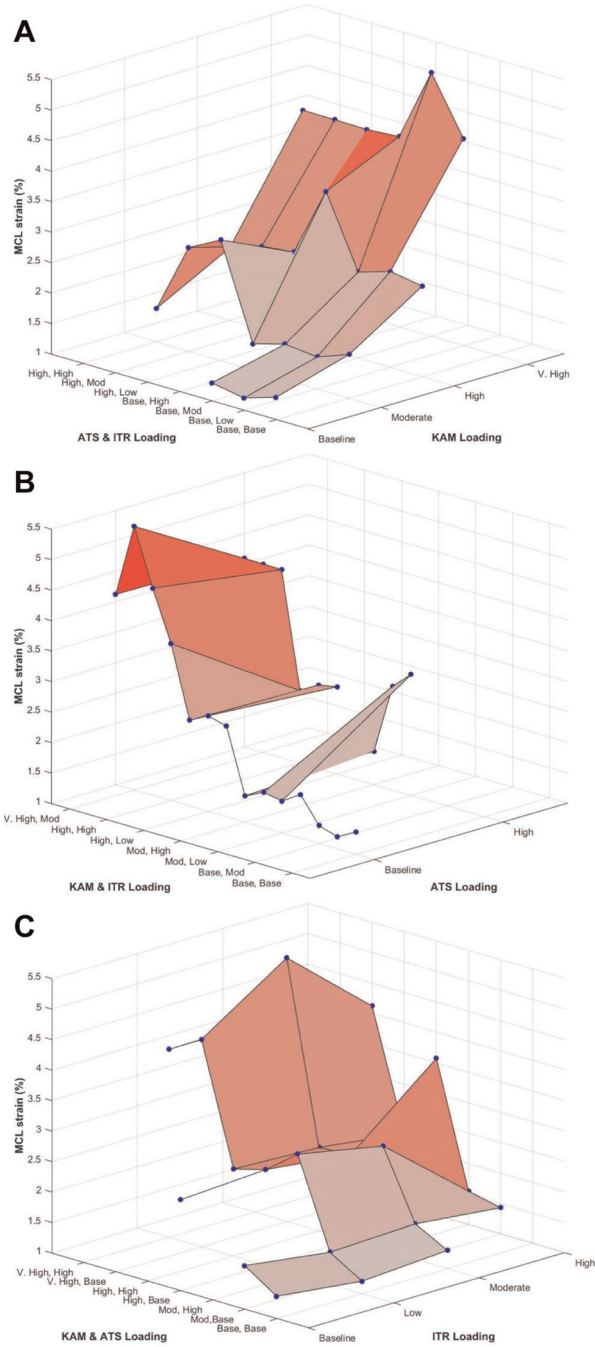


**Figure 4.** Heat maps depict how (A) KAM, (B) ATS, and (C) ITR individually influence absolute MCL strain relative to each combination of the other 2 loading conditions. The highest strains are observed when the KAM loading condition is in the very-high-risk state. Note that for each plot, the effect of the isolated loading factor is observed along the tertiary (*y*) axis, while the remaining combinatorial loading is depicted along the primary (*x*) axis. Moving from left to right along the tertiary axis on each plot, KAM affects a steeper

increase in strain than ATS or ITR. ATS, anterior tibial shear; ITR, internal tibial rotation; KAM, knee abduction moment; MCL, medial collateral ligament.

Author Manuscript

Author Manuscript

Author Manuscript

Author Manuscript

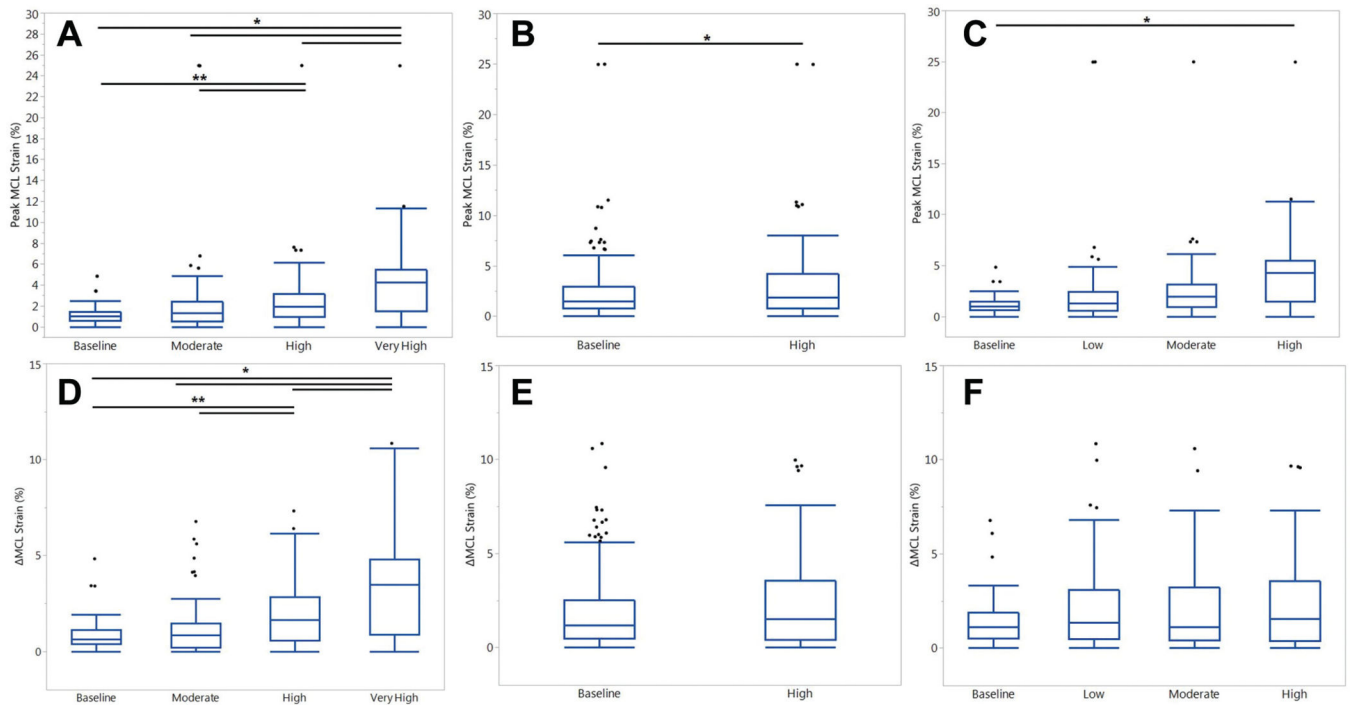


**Figure 5.**

Box plots with medians and interquartile ranges for MCL strain from all trials, separated by risk level for each loading factor: (A) KAM, (B) ATS, and (C) ITR. Means and SDs for DMCL strain from all trials, separated by risk level for each loading factor: (D) KAM, (E) ATS, and (F) ITR. Horizontal bars at the superior aspect of the graph indicate significant difference ( $P < .05$ ) between the 2 risk levels. Error bars indicate 95% CI, and circles indicate outliers. \* $P < .05$ . \*\* $P < .01$ . ATS, anterior tibial shear; ITR, internal tibial rotation; KAM, knee abduction moment; MCL, medial collateral ligament.

**TABLE 1**  
Externally Applied Loads for the Mechanical Impact Simulator Based on the In Vivo Cohort<sup>a</sup>

Risk Classification	KAM			ATS			ITR		
	In Vivo Cohort, Percentile	Load, N m	In Vivo Cohort, Percentile	Load, N m	In Vivo Cohort, Percentile	Load, N m	In Vivo Cohort, Percentile	Load, N m	
Baseline	2	2.4	0	40	0	1.0	0	1.0	
Low					33	9.7	33	9.7	
Moderate	68	27.0			67	18.6	67	18.6	
High	99	53.6	90	98	100	53.7	100	53.7	
Aggressive	200	114.6							

<sup>a</sup> ATS, anterior tibial shear; ITR, internal tibial rotation; KAM, knee abduction moment.



**TABLE 2**Each Potential Simulation Loading Configuration per Specimen<sup>a</sup>

Condition	Loading Parameter		
	KAM	ATS	ITR
1	Baseline	Baseline	Baseline
2	Baseline	Baseline	Low
3	Baseline	Baseline	Moderate
4	Baseline	Baseline	High
5	Baseline	High	Low
6	Baseline	High	Moderate
7	Moderate	Baseline	Baseline
8	Moderate	Baseline	Low
9	Moderate	Baseline	Moderate
10	Moderate	Baseline	High
11	Moderate	High	Low
12	Moderate	High	Moderate
13	Moderate	High	High
14	High	Baseline	Baseline
15	High	Baseline	Low
16	High	Baseline	Moderate
17	High	Baseline	High
18	High	High	Low
19	High	High	Moderate
20	High	High	High
21	Very high	Baseline	Low
22	Very high	Baseline	Moderate
23	Very high	Baseline	High
24	Very high	High	Low
25	Very high	High	Moderate
26	Very high	High	High

<sup>a</sup>ATS, anterior tibial shear; ITR, internal tibial rotation; KAM, knee abduction moment.